Supplement of

Interferences caused by the biogeochemical methane cycle in peats during the assessment of abandoned oil wells

Sebastian F. A. Jordan[1]*, Stefan Schloemer[1], Martin Krüger[1], Tanja Heffner[2], Marcus A. Horn[2], Martin Blumenberg[1]*

[1]Federal Institute for Geosciences and Natural Resources (BGR), Hannover, Stilleweg 2, 30655, Germany
[2]Leibniz Universität Hannover, Institute for Microbiology, Herrenhäuser Str. 2, Hannover, 30419, Germany

Correspondence to: Sebastian F. A. Jordan (Sebastian.Jordan@bgr.de), Martin Blumenberg (Martin.Blumenberg@bgr.de)

S1 Methane emission flux measurements

The smart chamber calculates the r^2 after the measurement and in our case, the majority of measurements had an r^2 above 0.5. From the measurements with $r^2 < 0.5$ the vast majority were fluxes around zero CH_4 flux with a range of ± 0.1 nmol m^{-2} s^{-1}. For a better understanding, we added three measurements below with fluxes of a) ~ -0.187 nmol m^{-2} s^{-1}, b) ~ 0.019 nmol m^{-2} s^{-1}, c) ~ 103.73 nmol m^{-2} s^{-1}.

(a)

	C_o		C_x		a		t_o
	2019.10455		0		0.00002		0
	dC/dt	SE of dC/dt	r^2	Flux	Flux CV		
Exponential	-0.03228	0.00063	0.97086	-0.18681	2.22349		
Linear	-0.03228	0.00063	0.97086	-0.18681	2.22349		

(b)

	C_o		C_x		a	t_o
	2015.13409		1000000		0	0
	dC/dt	SE of dC/dt	r^2	Flux	Flux CV	
Exponential	0.00336	0.00067	0.24529	0.01912	19.88846	
Linear	0.00336	0.00067	0.24529	0.01912	19.88846	

(c)

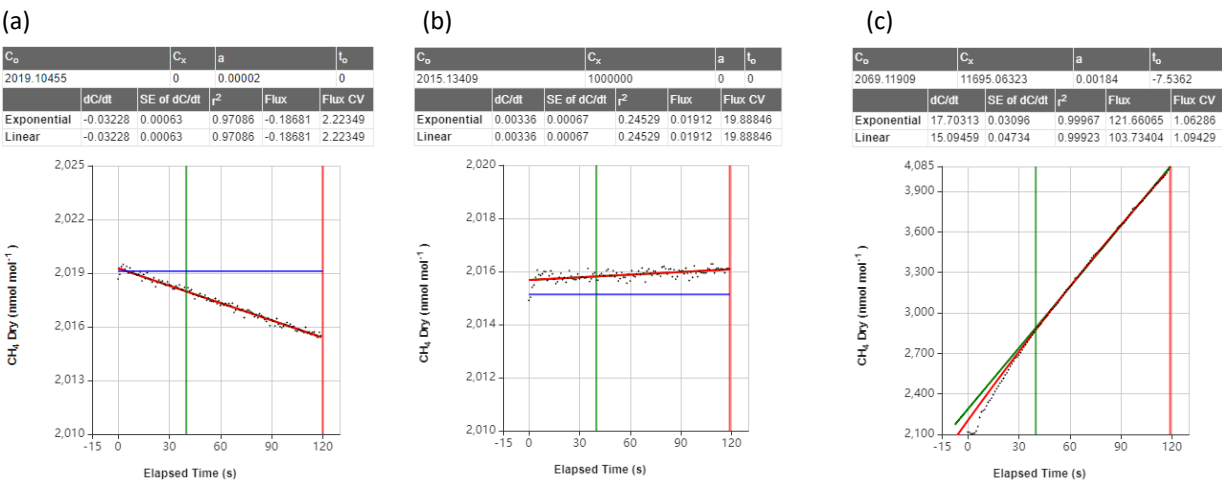|	C_o		C_x		a		t_o
	2069.11909		11695.06323		0.00184		-7.5362
	dC/dt	SE of dC/dt	r^2	Flux	Flux CV		
Exponential	17.70313	0.03096	0.99967	121.66065	1.06286		
Linear	15.09459	0.04734	0.99923	103.73404	1.09429		

Figure S1: Flux measurements using the cavity enhanced absorption spectroscopy trace gas analyzer (LI-COR 7810) coupled to a portable hydraulic chamber (LI-COR smart chamber). Displayed are three measurements with fluxes of a) ~ -0.187 nmol m^{-2} s^{-1}, b) ~ 0.019 nmol m^{-2} s^{-1}, c) ~ 121.66 nmol m^{-2} s^{-1}. The blue horizontal line depicts the measuring time which started with the closure of the chamber at 0 s, whereas the vertical lines indicate the end of the dead band (green) and the end of measurement and opening of the chamber (red). The exponential regression (bright red) and linear regression (orange) are depicted as well.

S2 Lipids after aerobic methane oxidation in the laboratory

28   It is well known that many methanotrophic bacteria of the Type I (γ-Proteobacteria) and Type II (α-Proteobacteria) cluster consist of specific phospholipid fatty acids (PLFA) with Type I mainly consisting of 14 and 16 carbon atoms and Type II of

30   18 carbon atom PLFA (e.g., Bodelier et al. (2009) and references therein). Furthermore, many of the methanotrophic bacteria in these Type clusters contain signature PLFA with C16:1Δ8c and C16:1Δ11t (or C16:1ω8c and C16:1ω5t, respectively)

32   specific for Type I and C18:1Δ10c or C18:1ω8c for type II (Bowman et al., 1991; Nichols et al., 1985). This classification was, however, challenged by findings of the Type I specific 16:1ω8 (together with an abundant 18:1ω8) in the Type II

34   methanotroph *Methylocystis heyeri* (Dedysh et al., 2007). *Methylocystis* are demonstrated to be abundant at Northern Europe, acidic peatlands (Dedysh, 2009) like e.g. Steimbke. In concordance to these studies, *Methylocystis* were indeed prominent in

36   our phylogenetic data of the peat organic matter used for this study from Steimbke (sample 7468) prior and after the lab experiment. Furthermore, all Type II methanotrophic *Beijerinckia* species lack the classical 18:1ω8 PLFA (Knief, 2015 and

38   reference therein). The differentiation between Type I and II methanotrophs is therefore complicated, while the presence of ω8 unsaturated PLFA in general remain a strong hint to methanotrophic bacteria.

40

Material & Methods

42   Peat soil samples taken in 2022 at Steimbke, two samples from the Meadow and Peat sites both with underlying peat, and two other sites for comparison were incubated with about 1–2% methane in air for a duration of 22 hours up to 58 days (see Table

44   S1). Four experiments were analyzed for changes in the lipid composition in the course of the experiments. The following samples were processed:

46

Table S1: Experiments analyzed for lipid changes during the course of methane addition (prior and after the experiments). Samples originate from the Peat site near Steimbke and the Nienhagen oil field

ID	origin	time [h]	MOx activity	MOx rate [μmol g^{-1} d^{-1}]
7468	Rodewald WA-272 (Steimbke peat extraction site), 10–15 cm	3	high	200
7470	Rodewald WA-275 (Steimbke meadow/peats) , 10–15 cm	22.5	low	5
7732	Carolinenhall, Nienhagen oil field, 10–15 cm	~1400	None	0
7734	Carolinenhall, Nienhagen oil field, 10–15 cm	~1400	none	0

All samples were subjected to alkaline hydrolysis to cleave intact phospho- and glycolipids using a method slightly modified after e.g., Oppermann et al. (2010). Briefly, 5 g soil samples were subjected to 6% KOH in methanol (MeOH) in excess for 2 h at 80°C in a screwed glass centrifuge tube. The resulting neutral lipids (NL) were extracted with *n*-hexane and were further separated into fractions of increasing polarity (hydrocarbons, ketones/aldehydes, alcohols, polar rest). Prior of the analysis, the alcohols were silylated with N,O-bis(trimethylsilyl)trifluoroacetamide (BSTFA). Acids extracted from the acidified residue after KOH-methanol hydrolysis, were transferred into their fatty acid methyl esters (FAME) in a screwed vial using trimethylchlorosilane (TMCS in MeOH 1:9; v:v; 2 h; 80 °C) and the combined extracted *n*-hexane phases (3x) were then, in addition to hydrocarbon, ketone/aldehyde and alcohol (BSTFA treated) fractions, analyzed with a GC-MS. The GC-MS comprised of an Agilent-7890 gas chromatograph equipped with a Programmable Temperature Vaporizing inlet splitting on two 50 m DB-1 columns (Agilent; 0.2 mm inner diameter; 0.11 μm film thickness), coupled to an FID and to an Agilent 7000 QQQ MS, each. Helium was used as carrier gas. MS-measurements were carried out in full scan mode. Compounds were identified by mass spectra and retention times in comparison with measurements of standard compounds. Here, only the acid fractions are presented and for simplification are named phospholipid fatty acids or "PLFA", which make up the main compounds in fresh soil samples after alkaline hydrolysis. Position of double bonds were determined after GC-MS analyses of DMDS derivatives of FAME using a method modified after Buser et al. (1983) and Gatellier et al. (1993). Details can be found elsewhere (Berndmeyer et al., 2013).
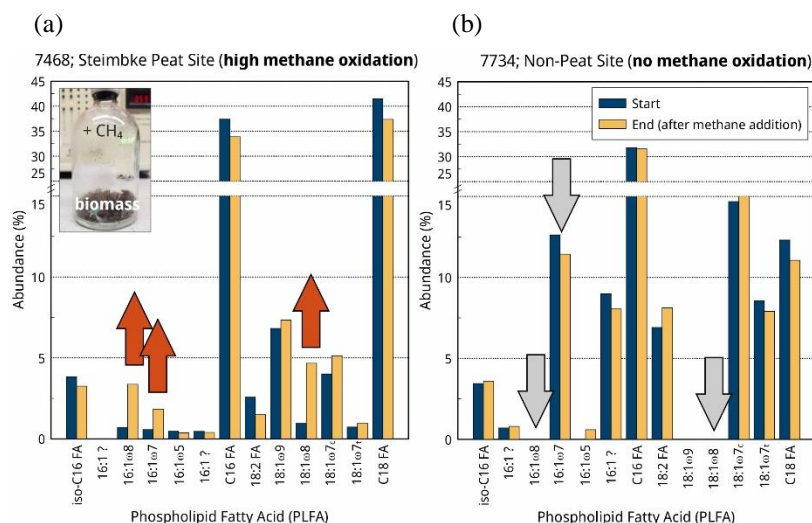
Results and Discussion

Fatty acids including hydrolyzed acids from phospho- and glycolipids remained relatively similar in all experiments (Figure S1). For better comparison the relative changes were visualized from normalizing the (short chain) fatty acid composition to the eicosanoic acid methyl ester, which was assumed to remain unchanged as this likely originates from plant litter (and not microbial lipids). However, some peaks (three specific unsaturated C16 and C18 fatty acids marked with an arrow in (Figure S1) increased in the course of one experiment, where methane oxidation rate was high (7468). These compounds were mostly

absent in other experiments and did also not change in those experiments after methane-addition. Further analyses of the double

76 bond positions revealed C16:1ω8c and C18:1ω8 (and, less specific, 16:1ω7), which are specific to methanotrophic bacteria. Normalized to 100% of FAMEs shown in Fig. S1 (without C20:0) C16:1ω8 increased in the experiment 7468 (peat site) from

78 0.69 to 3.37% and C18:1ω8 from 0.95 to 4.67%. Also C16:1ω7 increased slightly in abundance from 0.57 to 1.26%. This compound is abundant in the other experiment samples as well, but remained unchanged there. Thus, it appears less specific.

80 C16:1ω8 and C18:1ω8 are the most abundant PLFA in *Methylocystis heyeri* (Dedysh et al., 2007) and a *Methylocystis*-origin is in line with our phylogenetic data.

82 Although changes are specific to methanotrophic bacteria, changes in the PLFA (and free fatty acids) are relatively minor. This, however, is not uncommon and even occurs in highly active samples and can be explained by the high (non-

84 methanotrophic) load of microbial and plant organic matter in the original soil (peat) samples Knoblauch et al. (2008) and the likely generally relatively low abundance of methanotrophs among the microbial community in peat (Kaupper et al., 2021).

86 PLFA data are indicative of the presence of methanotrophic stemming PLFA in the original sample 7468, while respective biomarkers are lacking at the other sites. This evidences the presence of methanotrophic bacteria in the studied peats and the

88 presence of PLFA known from *Methylocystis*-relatives is in line with phylogenetic proofs of this group of MOB. In sample 7470, only very low methane oxidation was observed during the lab experiments compared to rates in samples 7468.

90 In addition, the methane concentrations in the original surrounding soil gases were much lower in 7470 than in 7468 (on average 9 ppm CH$_4$ and 24% CH$_4$, respectively). PLFA data were lacking proof of MOB in 7470 from Steimbke (prior and

92 after the experiment) as well as in other studied samples from another area in Lower Saxony (7732 and 7734).

94

Figure S2: Relative changes of fatty acids of selected samples after KOH-hydrolysis, indicating changes in the microbial community (and/or

98 heterogeneities in the samples). The samples originating from the peat site near Steimbke (7468) with high methane oxidation and the Nienhagen oil field (7734) where no methane oxidation activity was observed in the laboratory for comparison.

S3 Fractionation factor of aerobic methane oxidation in the laboratory

Materials & Methods

A peat soil sample (7644) taken in 2023 at Steimbke (depth: 10–25 cm) was incubated with about 3% methane in air. This sample was taken at the industrial peat site, where methane in the soil gas was highly concentrated. The sample, however, does not resemble that taken for the incubation experiments for PLFA analyses (7468). Three incubations were run in parallel and stopped after 24 h, 48 h, and 72 h (Table S2). Gases in the headspace of the vials were sampled and analyzed for gas composition and stable carbon isotopic signatures (for CH_4 and CO_2). Gas samples were analyzed with a refinery gas analyzer and carbon isotopes with a GC-IRMS. More details can be found in the main paper (sections 2.4).
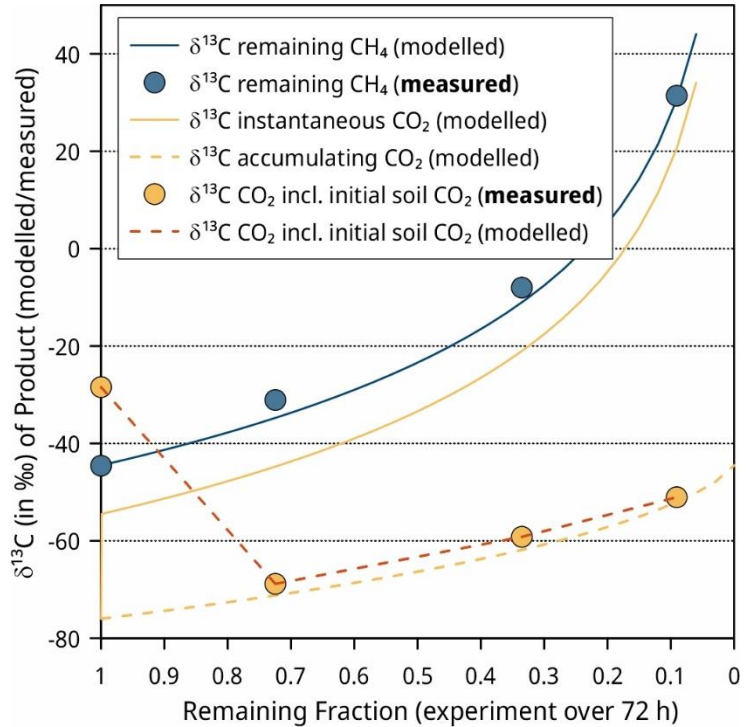
Table S2: Experimental isotope ($\delta^{13}C$) and concentration data of gases in the headspace after addition of methane (sample 7644; Steimbke peat). f = fraction of remaining methane after addition.

ID	time [h]	N_2 [%]	CH_4 [ppm]	CO_2 [ppm]	O_2 [ppm]	CH_4 [$\delta^{13}C$]	CO_2 [$\delta^{13}C$]	f	ε [‰]
7644	0	75.7	32,729	414	195,500	–44.58	–28.44	1.00	
7644	24	77.7	23,717	7811	170,001	–31.08	–68.84	0.72	
7644	48	79.9	10,974	14,513	156,917	–8.01	–59.18	0.34	
7644	72	81.1	2967	19,006	147,561	31.41	–51.05	0.09	
Enrichment factor									**–31.3**

Results & Discussion

Gas composition changed during the experiment with methane strongly and oxygen slightly de- and CO_2 increasing, typical for an experiment where methane is aerobically oxidized. At the same time, $\delta^{13}C$ values of CH_4 increased strongly, whereas $\delta^{13}C$ values of CO_2 decreased.

Figure S2 depicts the isotopic composition of the remaining methane, instantaneous and accumulating carbon dioxide as function of the fraction of the remaining methane (solid lines) assuming an initial zero CO_2 concentration. According to the mass and isotope balances at the time of the first experimentally measured $\delta^{13}C$-CO_2 value (at $f = 0.72$) the large amount of accumulating CO_2 (28% of ~3% added methane oxidized) with a cumulative $\delta^{13}C$-value of –71‰ easily shifts the original soil-derived, low concentrated (~414 ppm) and isotopically slightly depleted CO_2 ($\delta^{13}C$-CO_2 –28.4‰) towards very negative values (red dashed line).

Figure S3: Closed System Rayleigh fractionation (modelled (lines) and data (dots) of the experiment) of the incubation with methane and air.

126 After Elsner et al. (2007) and Feisthauer et al. (2011) the slope of plotting $\ln(\frac{(\delta_t+1000)}{\delta_0+1000})$ *versus* $\ln(\frac{c_t}{c_0})$ gives the enrichment factor ε (in‰; see Table S2 and Figure S3).
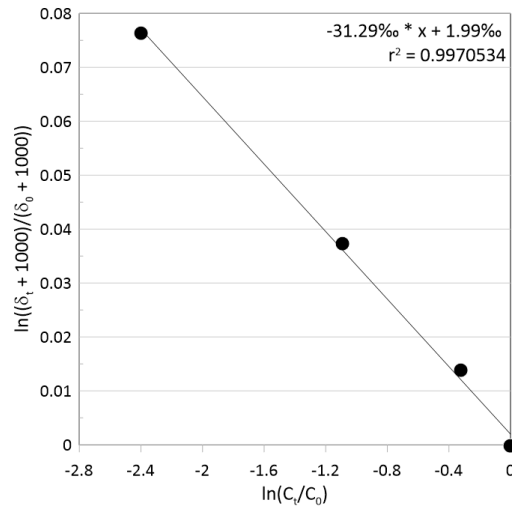
128

-31.29‰ * x + 1.99‰
$r^2 = 0.9970534$

$\ln((\delta_t + 1000)/(\delta_0 + 1000))$

$\ln(C_t/C_0)$

0.08
0.07
0.06
0.05
0.04
0.03
0.02
0.01
0

-2.8   -2.4   -2   -1.6   -1.2   -0.8   -0.4   0

Figure S4: Methane concentration and $\delta^{13}C$ change during the lab experiment 7644 (Steimbke peat). The slope (in ‰) corresponds to the enrichment factor ε (after Elsner et al. (2007) and Feisthauer et al. (2011)).
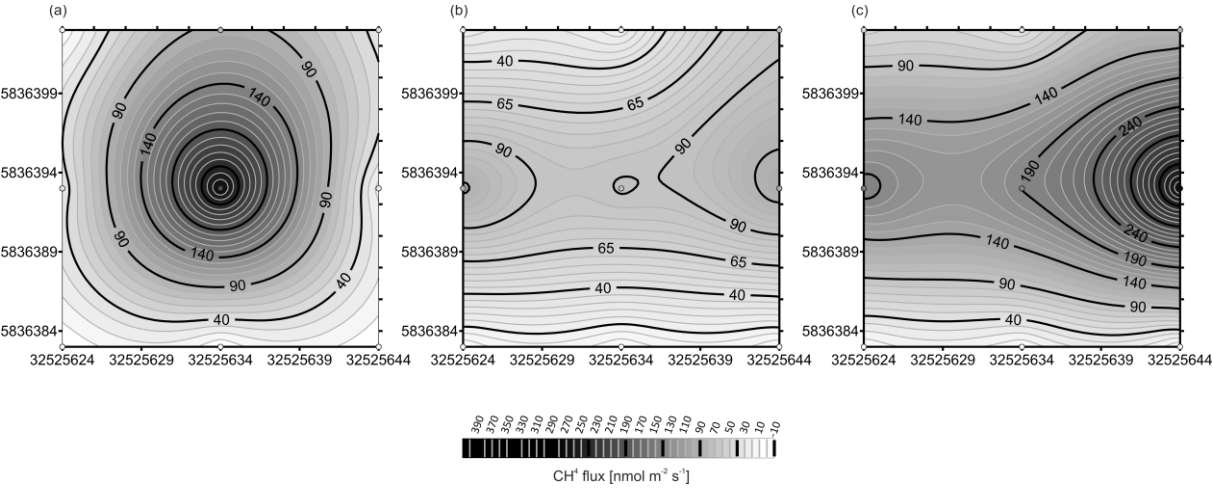
The calculated enrichment factor ε is with –31.3‰ (Figure S3) in the upper known range of data from laboratory experiments and cultures for aerobic methanotrophs (–3 to –39‰; Templeton et al. (2006) and references therein). It has to be considered that respective data are still limited, but the so far reported data demonstrate that a differentiation between the alpha- and gamma-proteobacteria or between the carbon assimilation pathway (Type I: assimilation of formaldehyde via the ribulose-monophosphate pathway; Type II: serine pathway) cannot be achieved from isotopic enrichment factors (Feisthauer et al., 2011; Rasigraf et al., 2012). In a comparative study highest fractionation factors were with –27.9 and –27.7‰, however, reported for the Type I methanotrophs *Methylococcus capsulatus* and *Methylomonas methanica* (Feisthauer et al., 2011). Our data and our lab enrichment culture dominated by members of the genera *Methylocystis* and *Methylobacter* add, however, further data on this still limited data set. Obviously, the isotopic fractionation of methane during aerobic methanotrophy at Steimbke results in a relatively strong fractionation. Reasons for this observation are, however, unclear. Previous studies speculated on the growth rates and physiological factors, and/or substrate limitation. Low oxygen concentrations may, theoretically, slow down methane oxidation by that favoring fractionation (Rasigraf et al., 2012; Templeton et al., 2006).

S4 Methane flux data

148

150   **Figure S5:** Gridding of methane fluxes from soil to the atmosphere at one reference site (a, b, c), which was measured at different time points in the active peat cutting area. First on April 20, 2022 (a), and then one week later on two consecutive days (April 27, (b) and 28 (c),
152   2022) (see Table 1). The grey scale is depicted on the bottom right.

154

S5 References

156   Berndmeyer, C., Thiel, V., Schmale, O., and Blumenberg, M.: Biomarkers for aerobic methanotrophy in the water column of the stratified Gotland Deep (Baltic Sea), Org Geochem, 55, 103-111,
158   https://doi.org/10.1016/j.orggeochem.2012.11.010, 2013.

Bodelier, P. L., Gillisen, M. J., Hordijk, K., Damste, J. S., Rijpstra, W. I., Geenevasen, J. A., and Dunfield, P. F.:
160   A reanalysis of phospholipid fatty acids as ecological biomarkers for methanotrophic bacteria, ISME J, 3, 606-617, https://doi.org/10.1038/ismej.2009.6, 2009.

162   Bowman, J. P., Skerratt, J. H., Nichols, P. D., and Sly, L. I.: Phospholipid fatty acid and lipopolysaccharide fatty acid signature lipids in methane-utilizing bacteria, FEMS Microbio Lett, 85, 15-22,
164   https://doi.org/10.1111/j.1574-6968.1991.tb04693.x, 1991.

Buser, H. R., Arn, H., Guerin, P., and Rauscher, S.: Determination of double bond position in mono-unsaturated
166   acetates by mass spectrometry of dimethyl disulfide adducts, Anal Chem, 55, 818-822,
https://doi.org/10.1021/ac00257a003, 1983.

168   Dedysh, S. N.: Exploring methanotroph diversity in acidic northern wetlands: Molecular and cultivation-based studies, Microbiology, 78, 655-669, https://doi.org/10.1134/s0026261709060010, 2009.

170   Dedysh, S. N., Belova, S. E., Bodelier, P. L. E., Smirnova, K. V., Khmelenina, V. N., Chidthaisong, A., Trotsenko, Y. A., Liesack, W., and Dunfield, P. F.: *Methylocystis heyeri* sp. nov., a novel type II
172   methanotrophic bacterium possessing 'signature' fatty acids of type I methanotrophs, Int J Syst Evol Microbiol, 57, 472-479, 10.1099/ijs.0.64623-0, 2007.

174   Elsner, M., McKelvie, J., Lacrampe Couloume, G., and Sherwood Lollar, B.: Insight into Methyl tert-Butyl Ether (MTBE) Stable Isotope Fractionation from Abiotic Reference Experiments, Environ Sci Technol, 41, 5693-
176   5700, 10.1021/es070531o, 2007.

Feisthauer, S., Vogt, C., Modrzynski, J., Szlenkier, M., Krüger, M., Siegert, M., and Richnow, H.-H.: Different
178   types of methane monooxygenases produce similar carbon and hydrogen isotope fractionation patterns during methane oxidation, Geochim Cosmochim Ac, 75, 1173-1184, https://doi.org/10.1016/j.gca.2010.12.006, 2011.

180   Gatellier, J.-P. L. A., de Leeuw, J. W., Sinninghe Damsté, J. S., Derenne, S., Largeau, C., and Metzger, P.: A comparative study of macromolecular substances of a Coorongite and cell walls of the extant alga
182   *Botryococcus braunii*, Geochim Cosmochim Ac, 57, 2053-2068, https://doi.org/10.1016/0016-7037(93)90093-c, 1993.

184   Kaupper, T., Mendes, L. W., Harnisz, M., Krause, S. M. B., Horn, M. A., and Ho, A.: Recovery in methanotrophic activity does not reflect on the methane-driven interaction network after peat mining, Appl
186   Environ Microbiol, 87, https://doi.org/10.1128/AEM.02355-20, 2021.

Knief, C.: Diversity and Habitat Preferences of Cultivated and Uncultivated Aerobic Methanotrophic Bacteria
188   Evaluated Based on *pmoA* as Molecular Marker, Front Microbiol, 6, 1346, https://doi.org/10.3389/fmicb.2015.01346, 2015.

190   Knoblauch, C., Zimmermann, U., Blumenberg, M., Michaelis, W., and Pfeiffer, E.-M.: Methane turnover and temperature response of methane-oxidizing bacteria in permafrost-affected soils of northeast Siberia, Soil Biol
192   Biochem, 40, 3004-3013, https://doi.org/10.1016/j.soilbio.2008.08.020, 2008.

Nichols, P. D., Glen A, S., Antworth, C. P., Hanson, R. S., and White, D. C.: Phospholipid and
194   lipopolysaccharide normal and hydroxy fatty acids as potential signatures for methane-oxidizing bacteria, FEMS Microbiol Lett, 31, 327-335, https://doi.org/10.1111/j.1574-6968.1985.tb01168.x, 1985.

196   Oppermann, B. I., Michaelis, W., Blumenberg, M., Frerichs, J., Schulz, H. M., Schippers, A., Beaubien, S. E., and Krüger, M.: Soil microbial community changes as a result of long-term exposure to a natural CO_2 vent,
198   Geochim Cosmochim Ac, 74, 2697-2716, https://doi.org/10.1016/j.gca.2010.02.006, 2010.

Rasigraf, O., Vogt, C., Richnow, H.-H., Jetten, M. S. M., and Ettwig, K. F.: Carbon and hydrogen isotope
200   fractionation during nitrite-dependent anaerobic methane oxidation by *Methylomirabilis oxyfera*, Geochim
     Cosmochim Ac, 89, 256-264, http://dx.doi.org/10.1016/j.gca.2012.04.054, 2012.
202 Templeton, A. S., Chu, K.-H., Alvarez-Cohen, L., and Conrad, M. E.: Variable carbon isotope fractionation
     expressed by aerobic CH_4-oxidizing bacteria, Geochim Cosmochim Ac, 70, 1739-1752,
204   https://doi.org/10.1016/j.gca.2005.12.002, 2006.